

# Network formation by aza-Michael addition of primary amines to vinyl end groups of enzymatically synthesized poly(glycerol adipate)

Razan Alaneed,<sup>a,c</sup> Yury Golitsyn,<sup>b</sup> Till Hauenschild,<sup>a</sup> Markus Pietzsch,<sup>c</sup> Detlef Reichert<sup>b</sup> and Jörg Kressler<sup>a\*</sup>



## Abstract

A highly efficient approach for the synthesis of polyester-based networks via aza-Michael addition of primary amines to  $\alpha,\beta$ -unsaturated (vinyl) end groups of poly(glycerol adipate) (PGA) was achieved. By acylation of PGA with 6-(Fmoc-amino)hexanoic acid side chains via Steglich esterification, protected amine-functionalized PGA was obtained. This was followed by the removal of fluorenylmethyloxycarbonyl (Fmoc) protecting groups and the synthesis of PGA-based networks under catalyst-free conditions. The successful conjugate addition of primary amines to vinyl end groups and network formation were confirmed using  $^{13}\text{C}$  magic angle spinning NMR and Fourier transform infrared spectroscopy. Network heterogeneity and defects were quantitatively investigated using  $^1\text{H}$  double-quantum NMR spectroscopy. Finally, a hydrogel was prepared with potential biomedical applications.

Supporting information may be found in the online version of this article.

**Keywords:** poly(glycerol adipate); vinyl end groups; aza-Michael addition; network synthesis; gels

## INTRODUCTION

Polymer networks belong to an important class of polymeric materials with a broad range of industrial and biomedical applications. By definition, polymer networks are three-dimensional structures that can be formed by crosslinking of polymer chains, by either chemical or physical crosslinks.<sup>1-3</sup> Hydrophilic polymer networks can form hydrogels with tunable water uptake capacity. They have been used and developed for various biological and biomedical purposes.<sup>4-6</sup> Specifically, biodegradable and biocompatible hydrogel systems have attracted considerable interest for their use in drug delivery, as they offer a convenient controlled drug release. Therefore, it is advantageous to use biodegradable polymer backbones in the preparation of hydrogels.<sup>7</sup> Among these biodegradable polymers, aliphatic polyesters are receiving significant attention due to their biodegradability and biocompatibility that make them favorable candidates for drug delivery systems.<sup>8-10</sup> The traditional synthetic pathways for the production of polyesters use metal-based catalysts. Under these conditions, the residual metals from the catalyst used are hard to remove, which may have harmful effects on the environment as well as the resulting polyesters with metallic traces being not suitable for biomedical use due to their potential toxicity.<sup>11-13</sup> Hence, *in vitro* synthesis of polyesters through enzymatic polymerization in organic media has been extensively developed as an important

alternative to the conventional polycondensation or ring-opening polymerization because of the high catalytic activity and high selectivity of the enzymes under mild reaction conditions.<sup>14</sup> Aliphatic functional polyester synthesis using enzymes as biocatalysts is promising for environmentally benign synthesis of polymeric materials.<sup>15</sup> In this regard, the most widely used enzyme is lipase B derived from *Candida antarctica* (CAL-B). CAL-B shows high regioselectivity towards primary hydroxyl groups rather than secondary ones.<sup>16</sup> Thus, linear polyesters can be synthesized having pendant OH groups on their backbones, which renders these polymers hydrophilic. Poly(glycerol adipate) (PGA) is a well-established, hydrophilic polyester with one pendant free OH group per repeat unit. It is generally produced from

\* Correspondence to: J Kressler, Department of Chemistry, Martin Luther University Halle-Wittenberg, D-06099 Halle (Saale), Germany. E-mail: joerg.kressler@chemie.uni-halle.de

<sup>a</sup> Department of Chemistry, Martin Luther University Halle-Wittenberg, Halle (Saale), Germany

<sup>b</sup> Department of Physics, Martin Luther University Halle-Wittenberg, Halle (Saale), Germany

<sup>c</sup> Department of Pharmaceutical Technology and Biopharmacy, Institute of Pharmacy, Martin Luther University Halle-Wittenberg, Halle (Saale), Germany

enzymatic transesterification reaction between glycerol and either dimethyl adipate or divinyl adipate. PGA has been widely investigated in the field of drug delivery.<sup>17–19</sup> Likewise, our group has reported a modified PGA, which was synthesized from activated vinyl ester monomers with various fatty acids to produce amphiphilic PGA useful for nanoparticle formation.<sup>20</sup> Recently, the conjugation between dimethylcasein and amine-functionalized PGA using microbial transglutaminase was reported.<sup>21</sup>

In the work reported in this paper, we focused on the development of an efficient strategy for the synthesis of biodegradable and biocompatible networks. Initially, we synthesized PGA with well-defined vinyl end groups. Then, 6-(Fmoc-amino)hexanoic acid (6-(Fmoc-Ahx)) side chains were introduced to the PGA backbone to produce PGA-*g*-6-(Fmoc-amino)hexanoate (PGA-*g*-6-(Fmoc-Ahx)). The use of Fmoc (fluorenylmethyloxycarbonyl) as a protecting group is crucial in order to achieve well-defined networks in the final synthesis step. The Fmoc protecting groups were subsequently removed and the synthesis of networks based on PGA was achieved via aza-Michael addition reaction of primary nucleophilic amines to the vinyl end groups of the PGA backbone. This method is simple and works efficiently under mild conditions and without using any catalyst. The chemical structures were analyzed using Fourier transform infrared (FTIR), <sup>1</sup>H NMR and <sup>13</sup>C NMR spectroscopies. Gel permeation chromatography (GPC) and high-resolution matrix-assisted laser desorption ionization time-of-flight (HR MALDI-TOF) mass spectrometry were performed in order to determine the molar mass and polydispersity index. Special focus was given to the quantitative determination of vinyl end groups using <sup>13</sup>C NMR spectroscopy and HR MALDI-TOF mass spectrometry. Michael addition reaction was followed via the complete disappearance of vinyl end groups after network formation as estimated based on FTIR and <sup>13</sup>C single pulse (SP) magic angle spinning (MAS) NMR spectroscopic data. For the characterization of the network structure and free dangling chain ends, <sup>1</sup>H double-quantum (DQ) NMR spectroscopy was employed. Finally, a hydrogel with potential biomedical applications was synthesized.

## EXPERIMENTAL

### Materials

CAL-B immobilized on an acrylic resin (Sigma-Aldrich, St Louis, MO, USA), commercially known as Novozyme (N435), was dried over phosphorus pentoxide (P<sub>2</sub>O<sub>5</sub>) at 4 °C for 24 h prior to use. 6-(Fmoc-Ahx) (98%) was purchased from Alfa Aesar (Kandel, Germany). Divinyl adipate (DVA; stabilized with 4-methoxyphenol, >99.0%) was purchased from TCI-Europe. Tetrahydrofuran (THF; anhydrous, 99.5%) and dichloromethane (DCM; anhydrous, 99.9%) were purchased from Acros Organics (Schwerte, Germany). P<sub>2</sub>O<sub>5</sub> (≥99%), 4-(dimethylamino)pyridine (DMAP), 1-ethyl-3-(3-dimethylaminopropyl)carbodiimide hydrochloride (EDC-HCl), silica gel (SiO<sub>2</sub>; 0.03–0.2 mm), dimethylsulfoxide (DMSO)-*d*<sub>6</sub> (99.8%) and CDCl<sub>3</sub> (99.8%) were purchased from Carl Roth (Karlsruhe, Germany). Glycerol (≥99.5%), deuterium oxide (D<sub>2</sub>O; 99.9%) and anhydrous DMSO were obtained from Sigma-Aldrich (Steinheim, Germany). All chemicals were used as received without further purification. All HPLC-grade solvents like THF, ethyl acetate, *tert*-butylmethyl ether, diethyl ether and acetone were purchased from Carl Roth (Karlsruhe, Germany).

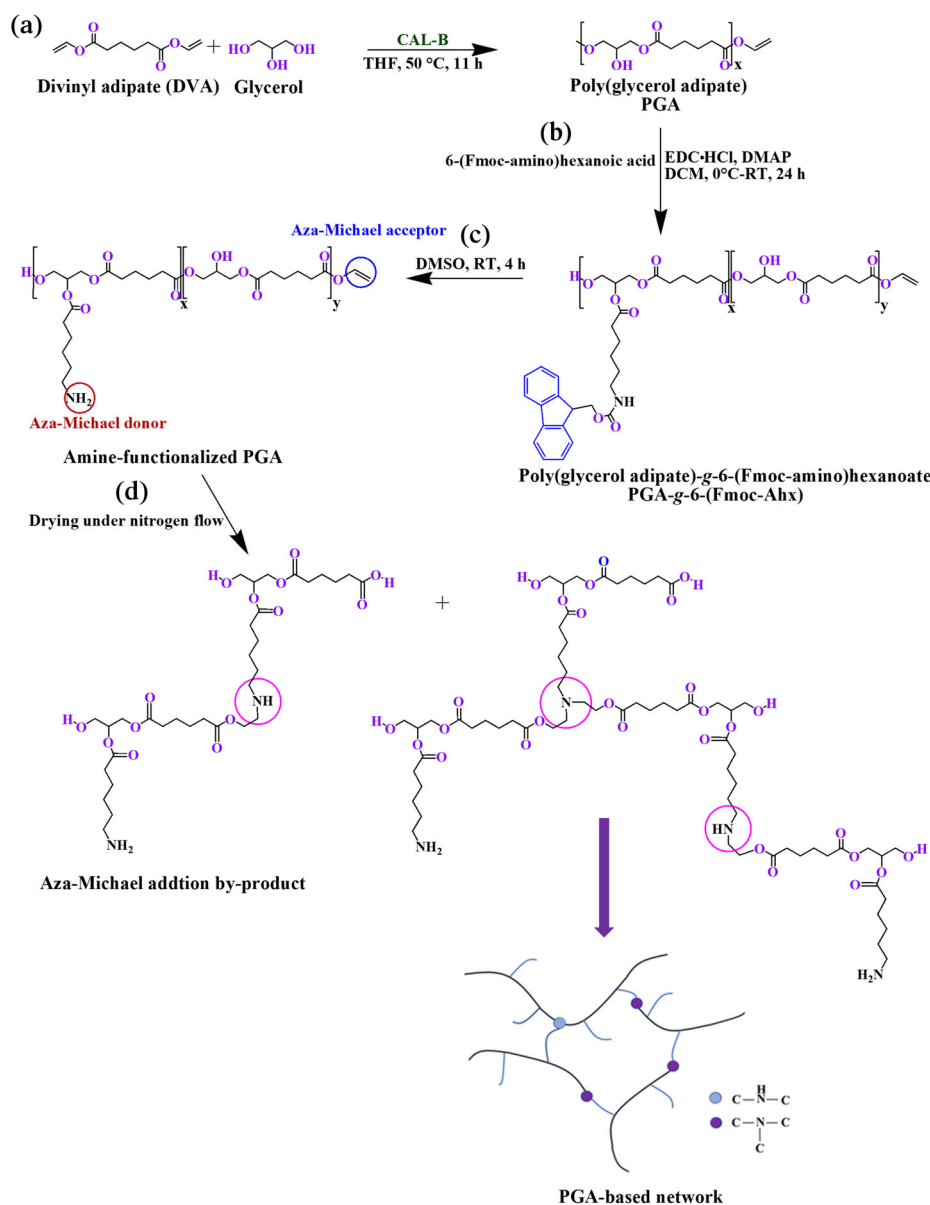
### Synthesis of PGA

PGA backbone was synthesized following the same procedure described by Kallinteri et al.<sup>17</sup> as shown in Scheme 1(A). Glycerol

and DVA were used in equimolar amounts in the presence of CAL-B. The amounts used for this reaction were as follows: glycerol (11 g, 120 mmol), DVA (23.8 g, 120 mmol), 23 mL of anhydrous THF and Novozyme (N435) (0.72 g, 2 wt% of the total monomers mass). The reaction was carried out for 11 h at 50 °C. At the end, the reaction was quenched by adding 50 mL of THF at room temperature, followed by filtration in order to remove the enzyme beads. The solvent was removed by rotary evaporation at 60 °C under vacuum. The polymer was used for further modification without any additional purification steps. The molar mass of PGA was determined using GPC in THF as  $M_n = 6000 \text{ g mol}^{-1}$  with a polydispersity index (PDI) of 1.8 and using HR MALDI-TOF mass spectrometry as  $m/z 5696.65 \text{ g mol}^{-1}$  with a repeat unit of  $m/z 202 \text{ g mol}^{-1}$ . The <sup>1</sup>H NMR spectrum of PGA is given in Fig. 1. <sup>1</sup>H NMR (400 MHz, CDCl<sub>3</sub>;  $\delta$ , ppm): 5.26 (m, 1H), 5.10 (m, 1H), 4.37–3.9 (m, 6H), 3.60 (dd,  $J = 11.5, 6.2 \text{ Hz}$ , 2H), 2.45–2.26 (m, 4H), 1.75–1.56 (m, 4H). IR (KBr;  $\nu$ , cm<sup>-1</sup>): 3470 ( $\nu$ (–OH)), 2953 ( $\nu_{\text{as}}$ (C–H)), 2875 ( $\nu_{\text{s}}$ (C–H)), 1726 ( $\nu$ (C=O)), 1646 ( $\nu$ (R–CH=CH<sub>2</sub>)), 1463 ( $\delta_{\text{s}}$ (C–H)), 1392–1280 (C–H ( $\omega, \tau$ )), 1264–1180 ( $\nu_{\text{as}}$ (C–O–C)), 1144–1080 ( $\nu_{\text{s}}$ (C–O–C)) and (C–H ( $\rho$ )), 1075–1055 ( $\delta$ (–OH)), 982–800 (C–H ( $\rho$ )), 980, 733 (R–CH=CH<sub>2</sub> ( $\gamma$ )).

### Synthesis of PGA-*g*-6-(Fmoc-Ahx)

PGA with a molar mass  $M_n$  of 6000 g mol<sup>-1</sup> was used for further modification with 6-(Fmoc-Ahx) according to the procedure described by Neises and Steglich,<sup>22</sup> shown in Scheme 1(B). PGA (1.5 g, 7.42 mmol) was dissolved in 20 mL of anhydrous DCM and then charged into a 100 mL three-neck round-bottom flask. The solution was cooled to 0 °C using an ice bath for 20 min. Then, a weighed amount of 6-(Fmoc-Ahx) (15 mol% of all OH groups, 0.4 g, 1.13 mmol) was added. Thereafter, weighed amounts of EDC-HCl (0.84 g, 4.4 mmol) and DMAP (40 mg, 0.33 mmol) were dissolved in 10 mL of anhydrous DCM and added dropwise. Under inert gas conditions, the reaction mixture was stirred for 24 h at room temperature. The reaction solution was filtered and the filtrate was concentrated to a volume of 4 mL using a rotary evaporator. The crude product was purified by silica gel column chromatography using HPLC-grade ethyl acetate as an eluent, in order to remove the unreacted 6-(Fmoc-Ahx), followed by HPLC-grade acetone which contained the grafted polymer. The solvent was removed using a rotary evaporator under reduced pressure. Further purification was done by precipitation into cold diethyl ether two times. After drying under vacuum at 35 °C, a slightly yellowish and viscous product was obtained. Product yield was 84 wt %. The molar mass of PGA-*g*-6-(Fmoc-Ahx) was calculated based on degree of grafting (mol%) from the <sup>1</sup>H NMR spectrum, given in Fig. 5, as  $M_n = 7000 \text{ g mol}^{-1}$ . The average molar mass of PGA-*g*-6-(Fmoc-Ahx) was also estimated using HR MALDI-TOF mass spectrometry as  $m/z 5739.72 \text{ g mol}^{-1}$  with a repeat unit of  $m/z 537.24 \text{ g mol}^{-1}$ . The PDI was determined using GPC in THF to be 1.7. <sup>1</sup>H NMR (400 MHz, CDCl<sub>3</sub>;  $\delta$ , ppm): 7.75 (d,  $J = 7.5 \text{ Hz}$ , 2H), 7.58 (d,  $J = 7.4 \text{ Hz}$ , 2H), 7.38 (t,  $J = 7.5 \text{ Hz}$ , 2H), 7.29 (t,  $J = 7.4 \text{ Hz}$ , 2H), 5.24 (q,  $J = 5 \text{ Hz}$ , 1H), 5.08 (q,  $J = 5 \text{ Hz}$ , 1H), 4.38–3.58 (m, 9H), 3.71 (s, 1H), 3.17 (q,  $J = 6.8 \text{ Hz}$ , 2H), 2.42–2.26 (m, 6H), 1.75–1.57 (m, 6H), 1.51 (s, 2H), 1.38–1.24 (m, 2H). IR (KBr;  $\nu$ , cm<sup>-1</sup>): 3470 ( $\nu$ (–OH)), 3455 ( $\nu$ (–NH)), 2953 ( $\nu_{\text{as}}$ (C–H)), 2875 ( $\nu_{\text{s}}$ (C–H)), 1726 ( $\nu$ (C=O)), 1646 ( $\nu$ (R–CH=CH<sub>2</sub>)), 1535 ( $\delta$ (–NH)), 1452 ( $\delta_{\text{s}}$ (C–H)), 1384–1280 (C–H ( $\omega, \tau$ )), 1260–1180 ( $\nu_{\text{as}}$ (C–O–C)), 1144–1075 ( $\nu_{\text{s}}$ (C–O–C)) and (C–H ( $\rho$ )), 1075–1055 ( $\delta$ (–OH)), 980, 733 (R–CH=CH<sub>2</sub> ( $\gamma$ )), 762, 733 (=C–H ( $\gamma$ )).



**Scheme 1.** Synthetic pathways for (a) PGA, (b) PGA-g-6-(Fmoc-Ahx), (c) deprotection of Fmoc groups and (d) aza-Michael addition byproduct and schematic representation of PGA-based network. The black chains correspond to PGA backbone with vinyl end groups and the blue chains correspond to the side chains that bear primary amine groups. A full presentation of PGA-based network structure is shown in the supporting information (Fig. S1).

### Deprotection of Fmoc groups and network formation

Fmoc protecting groups were removed applying the same method as described by Höck *et al.*,<sup>23</sup> with a slight modification. PGA-g-6-(Fmoc-Ahx) with a molar mass  $M_n$  of 7000 g mol<sup>-1</sup> (1 g, 1.86 mmol) was dissolved in 8 mL of anhydrous DMSO and the solution was agitated for 4 h at room temperature. To remove the formed byproduct, dibenzofulvene and most of DMSO, the polymer solution was precipitated twice into excess of cold *tert*-butylmethyl ether to yield amine-functionalized PGA (Scheme 1(C)). After drying under nitrogen flow for 30 min, 10 wt% of aza-Michael addition byproduct (sol content) and 90 wt% of yellowish PGA-based network were obtained as shown in Scheme 1(D). A schematic of the network is given in the supporting information (Fig. S1). This process occurred according to a typical Michael addition reaction since PGA has acceptor sites, i.e. vinyl end groups, in addition to the primary amine groups along the repeat units, which can act as aza-Michael donors. For network

characterization, the byproduct was dissolved again in DMSO and extracted from the network. IR (KBr;  $\nu$ , cm<sup>-1</sup>): 3482 ( $\nu$ (-OH)), 3387 ( $\nu$ (-NH)), 2941 ( $\nu_{as}$ (C-H)), 2871 ( $\nu_s$ (C-H)), 1737 ( $\nu$ (C=O)), 1651 ( $\delta_s$ (-NH<sub>2</sub>)), 1550 ( $\delta$ (N-H)), 1456 ( $\delta_s$ (C-H)), 1385–1280 (C-H ( $\omega$ , $\tau$ )), 1258–1170 ( $\nu_{as}$ (C-O-C)), 1144–1075 ( $\nu_s$ (C-O-C) and (C-H ( $\rho$ )), 1142, 1059 ( $\nu$ (C-N)), 759 (-NH<sub>2</sub> ( $\omega$ )). For <sup>1</sup>H DQ measurements, the network was swollen to equilibrium in DMSO-*d*<sub>6</sub>. In addition, the network was swollen in D<sub>2</sub>O in order to obtain hydrogels.

### Characterization

#### FTIR spectroscopy

FTIR measurements were performed with a Bruker Vector 22 FTIR spectrometer at room temperature with 256 scans using dry KBr for sample preparation. For all measurements, the sample concentration was 1.5 mg per 150 mg of KBr. FTIR spectral data were

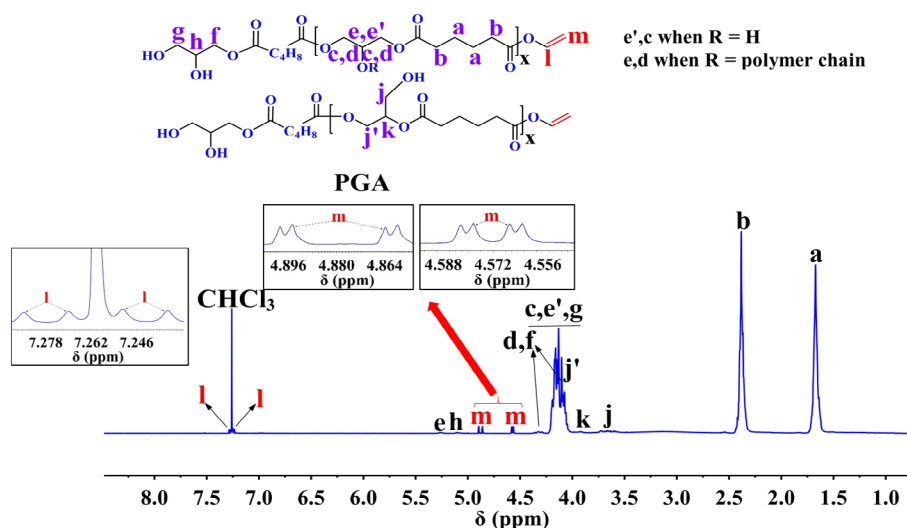


**Figure 1.**  $^1\text{H}$  NMR spectrum of PGA in  $\text{CDCl}_3$  at  $27^\circ\text{C}$ . The three insets show expansions of the peaks corresponding to vinyl end groups.

interpreted using OMNIC 7.2 Spectra software. All FTIR spectra were recorded in the range  $400\text{--}4000\text{ cm}^{-1}$ .

#### NMR spectroscopy

Solution NMR spectra ( $^1\text{H}$  NMR and  $^{13}\text{C}$  NMR) were recorded with a VNMRs spectrometer operating at 400 MHz for  $^1\text{H}$  NMR and 100 MHz for  $^{13}\text{C}$  NMR at  $27^\circ\text{C}$ , using an internal calibration standard, tetramethylsilane. Samples (*ca* 30 mg) were dissolved in 0.7 mL of deuterated solvents. The inversion-recovery method was performed in order to obtain the quantitative  $^{13}\text{C}$  NMR spectrum of PGA backbone by measuring the spin-lattice relaxation time ( $T_1$ ). For this, PGA sample (*ca* 300 mg) was dissolved in 0.7 mL of  $\text{CDCl}_3$ . The NMR spectral data were interpreted using MestRec (v.4.9.9.6) software (Mestrelab Research, Santiago de Compostela, Spain).

#### $^{13}\text{C}$ MAS NMR spectroscopy

$^{13}\text{C}$  SP MAS experiments were performed with a Bruker Avance 400 spectrometer at a frequency of 100.6 MHz, with a standard Bruker 4 mm MAS probe. A MAS spinning frequency of 10 kHz was applied in all experiments. Swollen network samples (in  $\text{DMSO-}d_6$  and  $\text{D}_2\text{O}$ ) were filled into a Bruker Kel-F MAS insert,<sup>24</sup> for liquid samples. The sample temperature was controlled with a standard Bruker VT controller and calibrated with methanol. The experimental temperature was regulated to  $30^\circ\text{C}$ . The  $^{13}\text{C}$  NMR  $\pi/2$  pulse length varied between 2.5 and 3.0  $\mu\text{s}$ . The recycle delay was set to 10 s for all samples.

#### $^1\text{H}$ DQ NMR measurements

$^1\text{H}$  DQ NMR experiments were run with a 200 MHz Bruker Avance III spectrometer using a static 5 mm Bruker probe with a short dead time (2.5  $\mu\text{s}$ ). The temperature was controlled with a BVT-3000 heating device with an accuracy of  $\pm 1^\circ\text{C}$  and was set to  $30^\circ\text{C}$  for all measurements. The  $^1\text{H}$  pulse length for the  $\pi/2$  and  $\pi$  pulses was set to 3.0 and 6.0  $\mu\text{s}$ , respectively. The sample was swollen to equilibrium in  $\text{DMSO-}d_6$  and  $\text{D}_2\text{O}$  at room temperature and the NMR tubes were sealed. The swelling ratio of PGA-based networks was measured after soaking the dried network in  $\text{D}_2\text{O}$  and in  $\text{DMSO-}d_6$  at room temperature for 24 h. The swelling ratio ( $Q$ ) can be calculated as follows:

$$Q = \frac{m_s - m_d}{m_d}$$

where  $m_s$  is the mass of swollen network and  $m_d$  represents the mass of dry network. The swelling ratio of PGA-based networks in  $\text{D}_2\text{O}$  and in  $\text{DMSO-}d_6$  was 4.8 and 8.5, respectively.

#### GPC measurements

GPC measurements for PGA and PGA-*g*-6-(Fmoc-Ahx) were performed with a Viscotek GPC max VE 2002 using HHRH Guard-17360 and GMHH-N-18055 columns and refractive index detector (VE 3580, Viscotek). THF was used as mobile phase in a thermostatically controlled column at  $25^\circ\text{C}$ . For both samples, the concentration was  $3\text{ mg mL}^{-1}$ , and the flow rate was  $1\text{ mL min}^{-1}$ . The calibration standard for both measurements was polystyrene. The data were analyzed using Origin 8 software.

#### MALDI-TOF mass spectrometry

The HR MALDI-TOF mass spectra were recorded with a REFLEX-TOF mass spectrometer (Bruker Daltonik GmbH, Bremen), equipped with a 337 nm nitrogen laser, which was operated at a pulse frequency of 3 Hz. The ions were accelerated using pulsed ion extraction after a delay of 50 ns by a voltage of 28.5 kV. The analyzer was operated in HR reflectron mode, and generated ions were detected with a microchannel plate detector. For calibration of the mass spectrometer, a polystyrene standard was used. The sample preparation for the recorded HR mass spectra was carried out by mixing of the samples (PGA and PGA-*g*-6-(Fmoc-Ahx)) with a suitable matrix, namely 2-[(2*E*)-3-(4-*tert*-butylphenyl)-2-methylprop-2-enylidene]malononitrile (DCTB), in a ratio of 1:1000 in THF. For preparing the sample, a stock solution of  $10\text{ mg mL}^{-1}$  DCTB in THF and  $10\text{ }\mu\text{g mL}^{-1}$  sample in the same solvent were used. Before the measurement, the prepared sample was crystallized on a stainless steel target. The resulting mass spectra were smoothed, and baseline-corrected with the XMASS data processing program (Bruker). mMass was used to evaluate the spectra. In a mass spectrum, the vertical  $y$ -axis represents the peak intensity (abundance of ions) and the horizontal  $x$ -axis represents the mass-to-charge ratio of the ions ( $m/z$ ). The molar mass of the ionized molecule was determined by the value of  $m/z$  ( $z = 1$ ).

## RESULTS AND DISCUSSION

### Enzymatic polymerization and grafting of PGA with 6-(Fmoc-Ahx) side chains

Enzymatic synthesis of PGA backbone can be achieved through transesterification reaction between glycerol and DVA in the presence of CAL-B. Although vinyl esters are considered to be more costly than alkyl esters (see supporting information), they are particularly suitable monomers for this synthesis as vinyl alcohol is released as a byproduct and tautomerizes promptly into acetaldehyde which can be removed easily at the reaction temperature making the reaction irreversible.<sup>25,26</sup> Thus, polymers with high molar mass are obtained. Compared to the use of dimethyl adipate instead of DVA in PGA synthesis, polymers with lower molar mass are produced.<sup>27</sup> Figure 1 presents the <sup>1</sup>H NMR spectrum of PGA synthesized from glycerol and DVA with peak assignments.

Analysis of the <sup>1</sup>H NMR spectrum shows characteristic signals of PGA, i.e. the methylene and methine proton signals, corresponding to the substituted glyceride and adipate units. Since the enzyme active site contains bound water molecules, which are crucial for enzyme activation, most vinyl end groups are hydrolyzed into carboxylic acid end groups during the polymerization reaction,<sup>28</sup> and some remain and can be recognized as three signals in the <sup>1</sup>H NMR spectrum at 7.29, 4.86 and 4.56 ppm as shown in the insets of Fig. 1. The methylene protons of vinyl end groups, labelled as (m), show two doublet of doublets at 4.86 and 4.56 ppm due to the unequal proton–proton coupling constants.

Although the enzyme shows high reactivity towards primary hydroxyl groups rather than secondary ones, some lack of enzyme regioselectivity is observed by the presence of several methine proton signals.<sup>29</sup> Kline *et al.*<sup>30</sup> reported the high reactivity of lipase towards primary OH groups (*ca* 95%) compared to secondary ones at 50 °C. These investigations explain the formation of differently substituted glyceride units, i.e. 1,2-disubstituted and 1,2,3-trisubstituted glyceride units in addition to 1,3-disubstituted and 1-substituted glyceride units that would

occur in the case of perfect enzyme regioselectivity towards primary OH groups. Similarly, our group has determined the regioselectivity of acylation of lipase toward primary OH groups as 96% in relation to secondary OH groups, which is highly dependent on the reaction temperature.<sup>31</sup> Additionally, PGA was analyzed using <sup>13</sup>C NMR spectroscopy. The spectrum reveals two signals at 141.2 and 97.9 ppm arising from vinyl end groups as can be seen in the inset of Fig. 2. The percentage of vinyl end groups was calculated quantitatively by the ratio of integrals between the adipate repeat unit carbons ( $\int a = 2$ ) and vinyl carbons at 97.9 ppm ( $\int m = 0.08$ ) to be estimated as 8% of the total end groups.

The molar mass and PDI of PGA were determined using GPC with THF as an eluent and polystyrene as calibration standard. The GPC traces are shown in the supporting information (Fig. S2). Along with GPC measurements, PGA was further analyzed using HR MALDI-TOF mass spectrometry in order to determine the absolute molar mass distribution. Figure 3 shows a representative HR MALDI-TOF mass spectrum of PGA molar mass distribution extending from *m/z* 4500 to *m/z* 7000, with a central intense peak at *m/z* 5696.65, which corresponds to the average molar mass of PGA. The HR MALDI-TOF mass spectrum is characterized by a number of peaks separated by regular intervals of *m/z* 202, which is the expected molar mass of PGA repeat units. This confirms the predominant linearity of PGA. The expanded view of the spectrum in the mass range *m/z* 5875–6050 reveals the presence of several series of peaks that can be assigned to different end groups of PGA chains, i.e. hydroxyl (OH) + H (18 + 202*n*), hydroxyl (OH) + vinyl (CH=CH<sub>2</sub>) (44 + 202*n*), adipate part + H (129 + 202*n*) and glycerol part + H (92 + 202*n*) terminated polymer chains wherein *n* is the number of repeat units per polymer chain. The highest intensity peak at *m/z* 5916.70 contains hydroxyl (OH) + H terminated polymer chains, which is in agreement with the PGA synthesis mechanism.

In the second step, side chains terminated with protected amine groups were introduced to the PGA backbone via Steglich

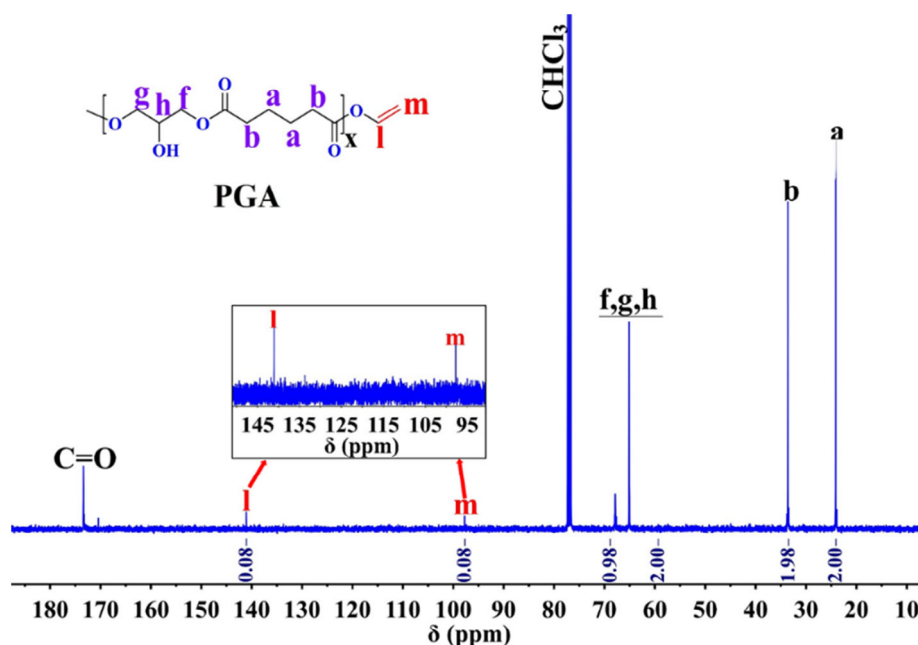


**Figure 2.** Quantitative <sup>13</sup>C NMR spectrum of PGA synthesized from DVA and glycerol in CDCl<sub>3</sub> at 27 °C. The inset shows an expansion of the peaks corresponding to vinyl end groups.

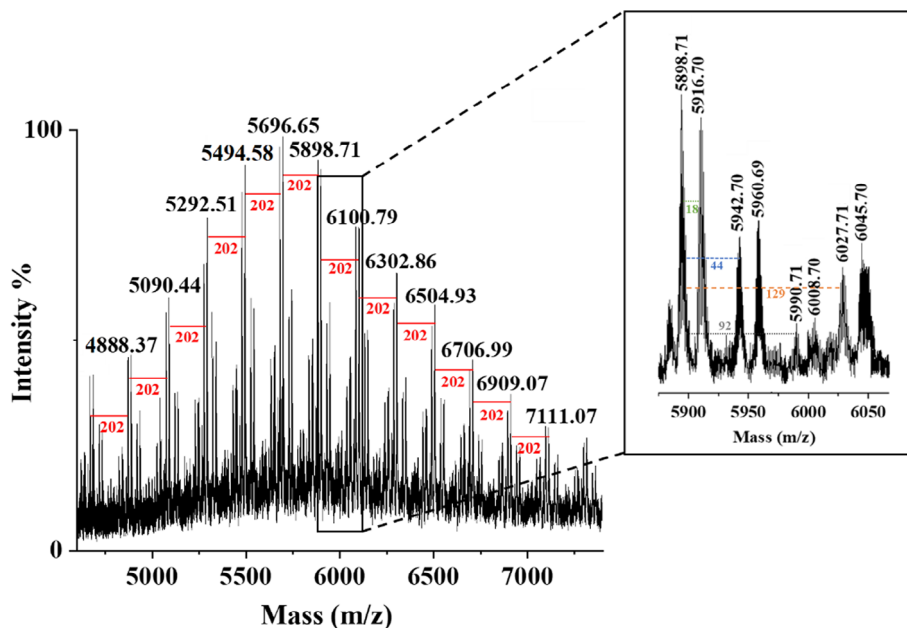


**Figure 3.** HR MALDI-TOF mass spectrum of PGA, using DCTB as a matrix. The molar mass of the repeat unit is  $202 \text{ g mol}^{-1}$ . The expanded view of the  $m/z$  5875–6050 region (right) shows different types of PGA end groups.

esterification between the secondary hydroxyl groups on PGA backbone and 6-(Fmoc-Ahx) with the help of DMAP as a catalyst and EDC-HCl as a coupling agent, as shown in Scheme 1(B). In addition, an excess of EDC-HCl was applied as a drying agent. The GPC traces, shown in the supporting information (Fig. S2), indicate that the grafted polymer has a higher molar mass than the unmodified PGA, indicating the successful acylation reaction. The molar mass and PDI of PGA and PGA-*g*-6-(Fmoc-Ahx) are given in the supporting information (Table S1). In addition to GPC measurements, PGA-*g*-6-(Fmoc-Ahx) was also investigated using HR MALDI-TOF mass spectrometry to determine the molar mass of the new repeat unit after modification. Figure 4 illustrates a full HR MALDI-TOF mass spectrum of the PGA-*g*-6-(Fmoc-Ahx) distribution in the range from  $m/z$  4600 to  $m/z$  7400. The expanded view in the mass range  $m/z$  5000–6750 in Fig. 4 shows the appearance of new peaks separated from the central intense peak by intervals of  $m/z$  537.24 due to the introduction of 6-(Fmoc-Ahx) side chains.

The chemical structure of PGA-*g*-6-(Fmoc-Ahx) was further confirmed using  $^1\text{H}$  NMR and  $^{13}\text{C}$  NMR spectroscopy. The  $^{13}\text{C}$  NMR spectrum is given in the supporting information (Fig. S3). The  $^1\text{H}$  NMR spectrum of PGA-*g*-6-(Fmoc-Ahx) is shown in Fig. 5. Analysis of the  $^1\text{H}$  NMR spectrum reveals the presence of proton signals, labelled with (n, o, p, q and r), which belong to the methylene protons of 6-(Fmoc-Ahx) side chains. The resonance of Fmoc (RNHC=O) proton, labelled with (s), appears as a weak and broad signal at 3.6 ppm. The resonance of aromatic rings labelled with (u, v, w, x and y), and the peak labelled with (t), reflect the protons of the Fmoc protecting group. The degree of grafting of OH groups of PGA is determined quantitatively using selective known peak integration represented in the corresponding  $^1\text{H}$  NMR spectrum. From the integrals of peaks (a) in the polymer backbone and (q) in the side chain, the degree of grafting (*g*) is calculated as 12 mol% with respect to all OH groups of the polymer backbone (where a theoretical value of 15 mol% grafting was used in the feed composition). The molar mass calculations are based on

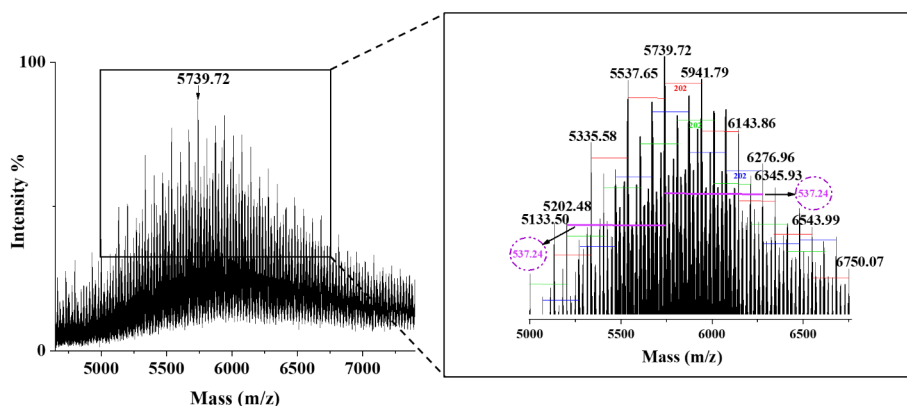


**Figure 4.** HR MALDI-TOF mass spectrum of PGA-*g*-6-(Fmoc-Ahx), using DCTB as a matrix. The expanded view in the mass range  $m/z$  5000–6750 (right) shows the molar mass of the new repeat unit as  $537.24 \text{ g mol}^{-1}$ .

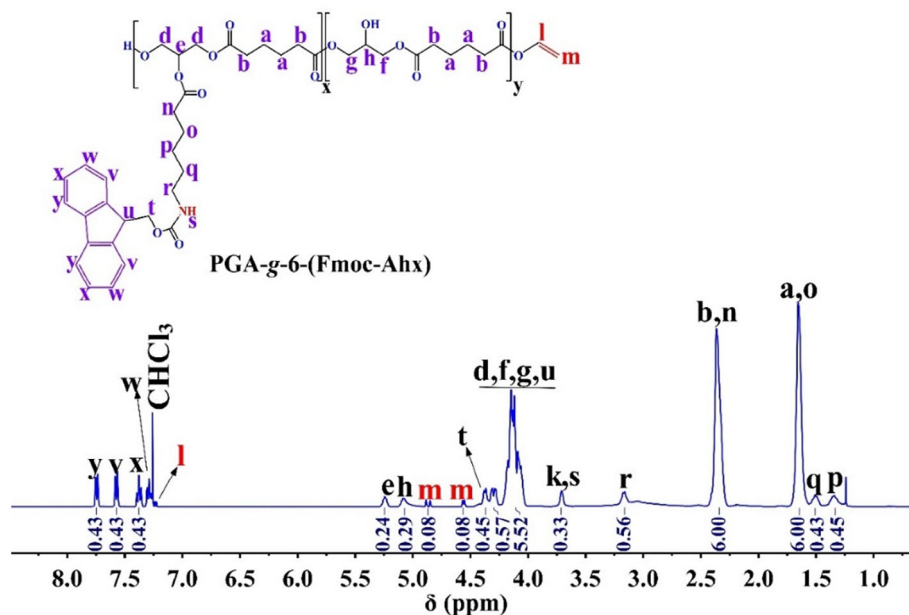


**Figure 5.**  $^1\text{H}$  NMR spectrum of PGA-g-6-(Fmoc-Ahx) in  $\text{CDCl}_3$  at  $27^\circ\text{C}$ .

$x$  to  $y$  ratio (given in the chemical structure of Fig. 5). Since  $y + x = 100\%$ , it follows that  $y = 88\%$  and  $x = g = 12\text{ mol}\%$ . Accordingly, the molar mass is calculated as  $7000\text{ g mol}^{-1}$ .

A comparison between the FTIR spectra of PGA and PGA-g-6-(Fmoc-Ahx) is shown in Fig. 6. For PGA, all major peaks are assigned. For instance, the spectrum shows a broad and strong peak for the hydroxyl ( $-\text{OH}$ ) stretching band at  $3470\text{ cm}^{-1}$  as a result of hydrogen bonds,  $\text{C}-\text{H}$  alkyl stretching bands between  $2953$  and  $2875\text{ cm}^{-1}$ , carbonyl ( $\text{C}=\text{O}$ ) stretching band at  $1726\text{ cm}^{-1}$  of the ester groups, vinyl end group stretching band at  $1646\text{ cm}^{-1}$ ,  $\text{C}-\text{H}$  bending between  $1463$  and  $1392\text{ cm}^{-1}$ , and  $\text{C}-\text{O}-\text{C}$  stretching bands between  $1264$  and  $1055\text{ cm}^{-1}$ .

After modification of PGA with 6-(Fmoc-Ahx), the stretching bands of  $-\text{OH}$ ,  $\text{C}-\text{H}$  and  $\text{C}=\text{O}$  are observed at the same wavenumber. The presence of ( $\text{RNHC}=\text{O}$ ) stretching band at  $3455\text{ cm}^{-1}$  which is overlapped with ( $-\text{OH}$ ) stretching band,  $\text{C}-\text{H}$  (aromatic) bands at  $762$  and  $743\text{ cm}^{-1}$  and amide II ( $-\text{NH}$ ) bending band at  $1535\text{ cm}^{-1}$  confirms the formation of PGA-g-6-(Fmoc-Ahx). Since the modification of PGA with 6-(Fmoc-Ahx)

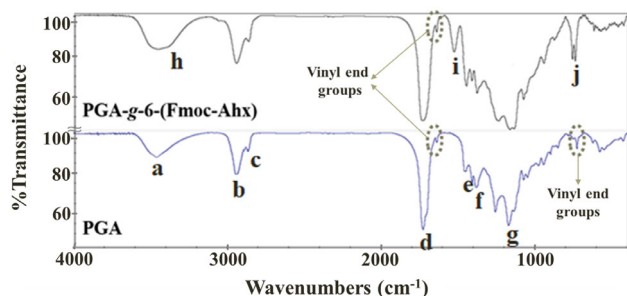


**Figure 6.** FTIR spectra of PGA and PGA-g-6-(Fmoc-Ahx) at room temperature. For PGA: (a)  $\text{OH}$  stretching,  $\nu(-\text{OH})$ , (b)  $\text{C}-\text{H}$  asymmetric stretching,  $\nu_{\text{as}}(\text{C}-\text{H})$ , (c)  $\text{C}-\text{H}$  symmetric stretching,  $\nu_{\text{s}}(\text{C}-\text{H})$ , (d)  $\text{C}=\text{O}$  stretching,  $\nu(\text{C}=\text{O})$ , (e)  $\text{C}-\text{H}$  scissoring bending,  $\delta_{\text{s}}(\text{C}-\text{H})$ , (f)  $\text{C}-\text{H}$  wagging and twisting,  $\text{C}-\text{H}$  ( $\omega$ ,  $\tau$ ), (g)  $\text{C}-\text{O}-\text{C}$  asymmetric and symmetric stretching,  $\nu_{\text{as,s}}(\text{C}-\text{O}-\text{C})$ . For PGA-g-6-(Fmoc-Ahx): (h)  $-\text{NH}$  stretching,  $\nu(-\text{NH})$ , (i) amide II bending,  $\delta(-\text{NH})$  and (j)  $=\text{CH}$  out-of-plane bending,  $=\text{CH}(\gamma)$ .

is only  $12\text{ mol}\%$ , i.e.  $x = g = 12\text{ mol}\%$  with respect to all  $\text{OH}$  groups of the polymer backbone, it can be observed that the stretching bands of ( $\text{C}-\text{H}$ ) alkyl chains and ( $\text{C}=\text{O}$ ) carbonyl of the ester groups become slightly sharper after this modification.

#### Deprotection of Fmoc protecting group

A mild method for the cleavage of Fmoc protecting group was applied under base-free conditions. This reaction was conducted in anhydrous DMSO and at room temperature, which resulted in a quantitative cleavage of Fmoc groups.<sup>23</sup> The cleavage process was monitored by increasing the olefin signal of the formed byproduct, dibenzofulvene, which appears in the  $^1\text{H}$  NMR spectrum as singlet at  $6.21\text{ ppm}$ , with the aromatic signals in the range  $7-8\text{ ppm}$ . The monitoring process of Fmoc cleavage was carried out in an NMR tube using deuterated DMSO. The  $^1\text{H}$  NMR spectrum is given in the supporting information (Fig. S4).

#### Network characterization

##### FTIR spectroscopy

PGA is a hydrophilic but water-insoluble linear polyester terminated with different end groups. Among them, some electron-deficient alkenes represent proper aza-Michael acceptors and can be involved in a nucleophilic addition reaction with free primary amines (aza-Michael donors),<sup>32-36</sup> to produce a hydrophilic polymer network under mild conditions. FTIR spectroscopy was used to investigate the network formation. Figure 7 depicts the FTIR spectrum of the PGA-based network, the structure of which is shown in Scheme 1(D). The complete disappearance of vinyl end group vibration band at  $1646\text{ cm}^{-1}$  after deprotection reaction and the appearance of  $\text{C}-\text{N}$  vibration band indicate the successful addition reaction of primary amines to vinyl end groups of the PGA backbone. In addition, the carbonyl  $\text{C}=\text{O}$  stretching band of the ester groups shifts to a higher wavenumber ( $1737\text{ cm}^{-1}$ ) due to electronegativity changes as all vinyl end groups disappear.<sup>37</sup> The presence of secondary and tertiary amine bands at  $1556$  and  $1059\text{ cm}^{-1}$ , respectively, represents the aza-Michael mono- and bis-addition products. The presence of primary amine

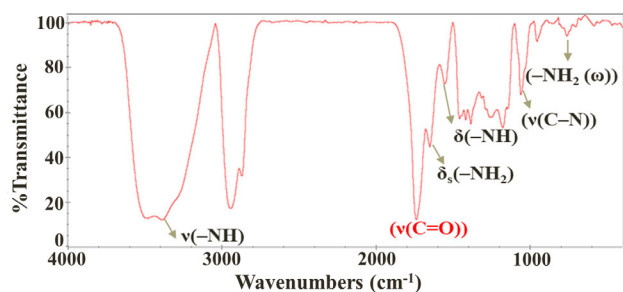


**Figure 7.** FTIR spectrum of PGA-based network at room temperature. Assignments ( $\text{cm}^{-1}$ ): 3387  $\nu(-\text{NH})$ , 1737  $\nu(\text{C}=\text{O})$ , 1651  $\delta_s(-\text{NH}_2)$ , 1550  $\delta(-\text{NH})$ , 1142, 1059  $\nu(\text{C}-\text{N})$ , 759  $-\text{NH}_2(\omega)$ . The spectrum shows the disappearance of vinyl end group vibration at  $1646\text{ cm}^{-1}$  after deprotection reaction and the appearance of  $(-\text{NH}_2)$  vibration band.

$(-\text{NH}_2)$  vibration bands explains that some free amine groups were not involved in the addition reaction.

### $^{13}\text{C}$ SP MAS spectra

$^{13}\text{C}$  SP MAS NMR measurements were performed in order to confirm the network structure. Figure 8 shows the  $^{13}\text{C}$  SP MAS spectrum of PGA-based network in  $\text{DMSO}-d_6$ . It is clearly visible that after network formation, there is no resonance arising from vinyl end groups in the regions of 141.2 and 97.9 ppm (shown in the inset of Fig. 8), which is in complete agreement with the FTIR results (Fig. 7).

Since the spectrum is well resolved, it is possible to determine the degree of grafting with 6-(Fmoc-Ahx) side chains. Therefore, the resonances labelled as (a), (b) and the carbonyl signal (C=O) which belong to the polymer backbone and the resonance labelled as (q) which is assigned to the side chain were integrated. All integration values and detailed calculations can be found in the supporting information. The degree of grafting represents the amount of the modified monomers  $x$  with 6-(Fmoc-Ahx) side chains. The degree of grafting is calculated as  $x = g = (9.8 \pm 5.0)\text{ mol}\%$  with respect to OH groups that corresponds well with the results of solution NMR spectroscopy. The  $^{13}\text{C}$  SP MAS spectrum of PGA-based network after swelling in  $\text{D}_2\text{O}$  is given in the supporting information (Fig. S5).

$^{13}\text{C}$  SP MAS NMR measurements together with FTIR results clearly demonstrate that the possibility of amine groups reacting with ester groups via amide formation is not relevant in our system. Since the reaction was carried out under mild conditions, it guarantees the stability of PGA.

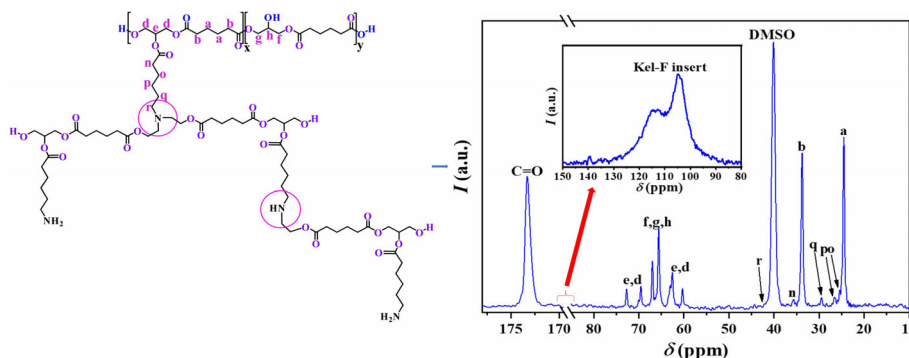


**Figure 8.**  $^{13}\text{C}$  SP MAS NMR spectrum of network swollen to equilibrium in  $\text{DMSO}-d_6$  measured at  $30\text{ }^\circ\text{C}$ . The inset shows the spectrum in the range 80 to 150 ppm. The broad signal corresponds to the sample insert,<sup>24</sup> but no vinyl resonances are present at 141.2 and 97.9 ppm.

### $^1\text{H}$ DQ NMR spectroscopy

The  $^1\text{H}$  DQ NMR experiment<sup>38</sup> provides information about the structure, defects and dynamics of polymer networks.<sup>39</sup> This method is able to describe systems with well-defined topology as well as systems with randomly distributed loop lengths.<sup>40,41</sup>

In the first step, the isotropically mobile uncoupled components, the so-called *tails*, are removed from the DQ signal. Figure 9(a) shows the procedure of the *tail* determination. Two components with significantly different decay times  $\tau$  could be identified. The component with the slow decay is assigned to the mobile *tail*, i.e. the mobile solvent molecules (non-deuterated solvent ca 13% of water, due to the hydrophilicity of the polymer backbone). The fast decaying component with 7% intensity corresponds to network defects such as loops and dangling chains, which are elastically inactive and do not contribute to the network structure. After subtraction of the two *tail* fractions and renormalization of the DQ data, the residual coupling constants (RDCs),  $D_{\text{res}}$ , can be estimated.<sup>39</sup>

Since the grafted side chains are randomly distributed along the polymer backbone, this can result in different mesh sizes, which means that the RDCs will also have a wide distribution according to the equation  $D_{\text{res}} \sim M_c^{-1}$ , where  $M_c$  is the chain molar mass between crosslinks or entanglements. In addition, the swollen elastomers always exhibit a broad  $D_{\text{res}}$  distribution, which is caused by inhomogeneous swelling and the resulting variations in local chain stretching.<sup>42</sup> The DQ data were directly evaluated with the help of a simultaneous fitting procedure:

$$I_{\Sigma\text{DQ}}(\tau_{\text{DQ}}) = \exp\left\{-\left(\tau_{\text{DQ}}/\tau\right)^\beta\right\} I_{\text{DQ}}(\tau_{\text{DQ}})$$

$$= \int_0^\infty I_{\text{DQ}}(\tau_{\text{DQ}}, D_{\text{res}}) p(D_{\text{res}}, \sigma) dD_{\text{res}} = \int_0^\infty \frac{1}{2} \left[1 - \exp\left\{-\left(0.378 \cdot D_{\text{res}} \tau_{\text{DQ}}\right)^{1.5}\right\} \cos(0.583 D_{\text{res}} \tau_{\text{DQ}})\right] \exp\left\{-\left(\tau_{\text{DQ}}/\tau\right)^\beta\right\} p(D_{\text{res}}, \sigma) dD_{\text{res}}$$

Fitting parameters are the time constant  $\tau$ , which corresponds to the characteristic decay time  $T_2^*$ , the exponent  $\beta$  of the Kohlrausch–Williams–Watts function, the RDC  $D_{\text{res}}$  and the width of the log-normal distribution  $\sigma$ . In the given formula, a log-normal distribution was used.



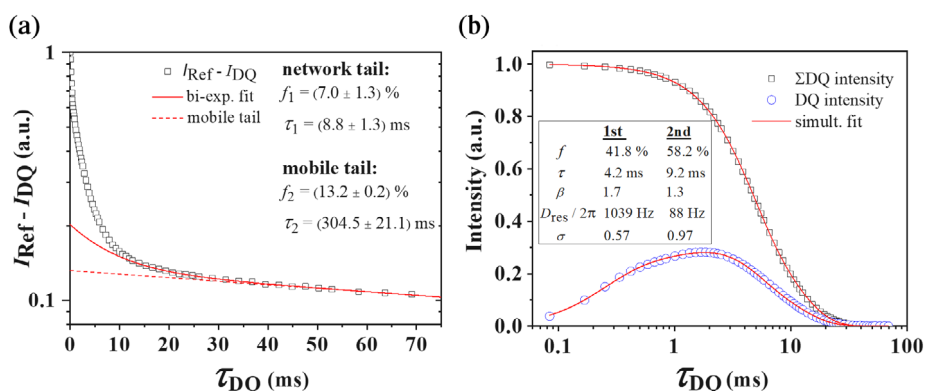


**Figure 9.** (a) Procedure of *tail* determination for the network, swollen to equilibrium in DMSO- $d_6$ . The red line represents the bi-exponential fit to the  $I_{\text{Ref}} - I_{\text{DQ}}$  intensity. The dashed line represents the mobile tail fraction. The fitting parameters are given in the inset. The fitting area begins at short time where the DQ intensity is already decayed and only a signal from the reference is present. (b) Simultaneous multicomponent fitting to the sum and DQ intensity after *tail* subtraction of the swollen-to-equilibrium network sample. The inset shows the fitting parameters. The component fractions  $f$  are given without taking into account the network *tail* of 7%.

According to the results in Fig. 9(b), we found two components arising from the elastic network structure. A comparison between the simultaneous fit with one and two network components in DMSO- $d_6$  is shown in the supporting information (Fig. S6(a)). These components are well separated due to the different relaxation times  $\tau$  and dipolar coupling constants  $D_{\text{res}}$ . Since the strength of the dipolar coupling decreases with increasing length of the network segment,<sup>43,44</sup> we can conclude that the first component with the larger coupling constant is the smallest possible mesh size. The second component represents larger mesh sizes and entanglements that make up the network. Taking the network *tail* into account, the composition of the sample is as follows: strongly coupled network component of 39%, weakly coupled network component of 54%, network defects of 7%. The existence of two well-distinguishable network components as well as the large distribution widths  $\sigma$  of the RDC indicate an inhomogeneous network structure, for example areas of high and low polymer concentration. The  $^1\text{H}$  DQ NMR data and the comparison between the simultaneous fit with one and two network components in  $\text{D}_2\text{O}$  are shown in the supporting information (Figs S7 and S6(b), respectively). Table S2 (supporting information) summarizes the results of the  $^1\text{H}$  DQ NMR data of PGA-based networks in DMSO- $d_6$  and  $\text{D}_2\text{O}$ .

To summarize, from the  $^{13}\text{C}$  SP MAS data it was possible to determine the degree of grafting of the modified PGA as  $(9.8 \pm 5) \text{ mol}\%$ . This corresponds to the value calculated from solution  $^1\text{H}$  NMR spectroscopy. With the help of the  $^1\text{H}$  DQ NMR measurements, the structure of the networks could be determined. Two

components with different RDC and large distribution widths were detected.

## CONCLUSIONS

We present a simple and catalyst-free approach towards the one-pot synthesis of polymer networks based on a biodegradable and biocompatible polyester, PGA. Initially, the lipase-catalyzed transesterification reaction between glycerol and DVA resulted in a hydrophilic polyester carrying  $\alpha,\beta$ -unsaturated (vinyl) end groups that acted as aza-Michael acceptors. In the next step, the pendant hydroxyl groups on the PGA backbone were partially modified by introducing protected amine-terminated side groups and the degree of grafting was calculated to be 10 mol% of total OH groups. It should be noted that grafting with non-protected amino acid leads to immediate but not well-defined network formation. The use of Fmoc as a protecting group offered the opportunity to generate a well-defined network in the final synthesis step. Subsequent removal of Fmoc protecting groups produced a modified PGA with side chains terminated with primary amine groups that served as aza-Michael donors resulting in polymer gelation and formation of a well-defined and hydrophilic network under mild reaction conditions in DMSO.

FTIR and  $^{13}\text{C}$  MAS NMR spectroscopic measurements confirm the network formation by the complete disappearance of vinyl end groups and the appearance of C—N bonds accordingly. Network heterogeneity and defects were determined using  $^1\text{H}$  DQ NMR spectroscopy in DMSO- $d_6$ , which reveals that two components form the elastic network structure, a strongly coupled network component of 39% and a weakly coupled network component of 54% with network defects of 7%. Besides, it was possible to perform the measurements in  $\text{D}_2\text{O}$  by removing DMSO from the synthesized networks and re-swelling in  $\text{D}_2\text{O}$ .  $^{13}\text{C}$  MAS NMR and  $^1\text{H}$  DQ NMR data of PGA-based networks in  $\text{D}_2\text{O}$  are presented in the supporting information that explain the presence of network components with lower coupling constant and shorter relaxation time comparing with the results obtained in DMSO- $d_6$  due to the poor water insolubility of the polymer backbone.

Figure 10 shows images of PGA-based hydrogels. It can be seen that the sample shows a high tack, which makes it suitable for typical pharmaceutical applications of hydrogels in combination with wet tissues. The tack properties of PGA-based hydrogels together

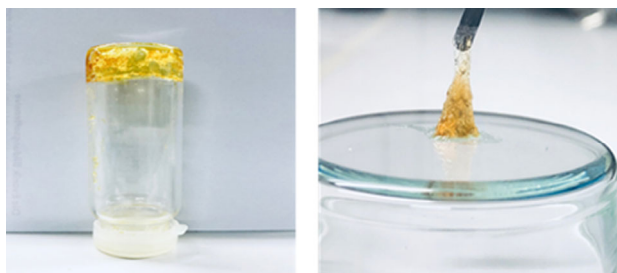


**Figure 10.** Appearance of PGA-based hydrogels.

with their biodegradability mean that they could have significant applications as barrier to prevent postoperative adhesions that may cause medical complications.<sup>45</sup>

Finally, the present protocol exhibits some significant benefits as being operationally simple, mild and catalyst-free, making it a promising approach for the synthesis of polyester-based networks with good water uptake capacity, which can be used for potential pharmaceutical applications such as carriers for sustained release of hydrophilic drugs<sup>46</sup> and biodegradable implants for controlled drug delivery.<sup>47</sup>

## ACKNOWLEDGEMENTS

This work was financially supported by Deutscher Akademischer Austauschdienst (DAAD) under a Research Grants – Doctoral Programs in Germany, 2017/18 (57299294). JK and DR thank Deutsche Forschungsgemeinschaft (JK 1714/9-2, RE 1025/19-2). Open access funding enabled and organized by Projekt DEAL.

## SUPPORTING INFORMATION

Supporting information may be found in the online version of this article.

## REFERENCES

- Dhandayuthapani B, Yoshida Y, Maekawa T and Kumar DS, *Int J Polym Sci* **2011**:1–19 (2011).
- Rezwan K, Chen QZ, Blaker JJ and Boccaccini AR, *Biomaterials* **27**: 3413–3431 (2006).
- Gu Y, Zhao J and Johnson JA, *Angew Chem Int Ed* **59**:5022–5049 (2020).
- Peppas NA and Khare AR, *Adv Drug Deliv Rev* **11**:1–35 (1993).
- Buwalda SJ, Vermonden T and Hennink WE, *Biomacromolecules* **18**: 316–330 (2017).
- Hirst AR, Escuder B, Miravet JF and Smith DK, *Angew Chem Int Ed* **47**: 8002–8018 (2008).
- Kamath KR and Park K, *Adv Drug Deliv Rev* **11**:59–84 (1993).
- Coulember O, Degée P, Hedrick JL and Dubois P, *Prog Polym Sci* **31**: 723–747 (2006).
- Jeske RC, DiCiccio AM and Coates GW, *J Am Chem Soc* **129**: 11330–11331 (2007).
- Amass W, Amass A and Tighe B, *Polym Int* **47**:89–144 (1998).
- Azim H, Dekhterman A, Jiang Z and Gross RA, *Biomacromolecules* **7**: 3093–3097 (2006).
- Cao H, Han H, Li G, Yang J, Zhang L, Yang Y et al., *Int J Mol Sci* **13**: 12232–12241 (2012).
- Jiang Y, Woortman AJ, van Ekenstein GO and Loos K, *Biomolecules* **3**: 461–480 (2013).
- Kobayashi S, *Proc Jpn Acad Ser B* **86**:338–365 (2010).
- Kobayashi S, Uyama H and Kimura S, *Chem Rev* **101**:3793–3818 (2001).
- Uyama H, Klegraf E, Wada S and Kobayashi S, *Chem Lett* **29**:800–801 (2000).
- Kallinteri P, Higgins S, Hutcheon GA, St Pourçain CB and Garnett MC, *Biomacromolecules* **6**:1885–1894 (2005).
- Wersig T, Hacker MC, Kressler J and Mäder K, *Int J Pharm* **531**:225–234 (2017).
- Swainson SME, Taresco V, Pearce AK, Clapp LH, Ager B, McAllister M et al., *Eur J Pharm Biopharm* **142**:377–386 (2019).
- Weiss VM, Naolou T, Hause G, Kuntsche J, Kressler J and Mäder K, *J Control Release* **158**:156–164 (2012).
- Alaneed R, Hauenschild T, Mäder K, Pietzsch M and Kressler J, *J Pharm Sci* **109**:981–991 (2020).
- Neises B and Steglich W, *Angew Chem Int Ed* **17**:522–524 (1978).
- Höck S, Marti R, Riedl R and Simeunovic M, *Chimia* **64**:200–202 (2010).
- Smernik RJ and Oades JM, *Solid State Nucl Magn Reson* **20**:74–84 (2001).
- Puskas JE, Seo KS and Sen MY, *Eur Polym J* **47**:524–534 (2011).
- Castano M, Seo KS, Guo K, Becker ML, Wesdemiotis C and Puskas JE, *Polym Chem* **6**:1137–1142 (2015).
- Naolou T, Weiss VM, Conrad D, Busse K, Mäder K and Kressler J, Fatty acid modified poly(glycerol adipate): polymeric analogues of glycerides, in *Tailored Polymer Architectures for Pharmaceutical and Biomedical Applications*, Vol. **1135**, ed. by Scholz C and Kressler J. American Chemical Society, Washington, DC, pp. 39–52 (2013).
- Chaudhary AK, Lopez J, Beckman EJ and Russell AJ, *Biotechnol Prog* **13**: 318–325 (1997).
- Taresco V, Suksiriworapong J, Creasey R, Burley JC, Mantovani G, Alexander C et al., *J Polym Sci A Polym Chem* **54**:3267–3278 (2016).
- Kline BJ, *J Am Chem Soc* **120**:9475–9480 (1998).
- Bilal MH, Hussain H, Prehm M, Baumeister U, Meister A, Hause G et al., *Eur Polym J* **91**:162–175 (2017).
- Rulev AY, *Russ Chem Rev* **80**:197–218 (2011).
- Yadav JS, Ramesh Reddy A, Gopal Rao Y, Narsaiah AV and Reddy BVS, *Lett Org Chem* **4**:462–464 (2007).
- Ying AG, Liu L, Wu GF, Chen G, Chen XZ and Ye WD, *Tetrahedron Lett* **50**:1653–1657 (2009).
- Reddick JJ, *Org Lett* **5**:1967–1970 (2003).
- Matveeva EV, Petrovskii PV and Odinetz IL, *Tetrahedron Lett* **49**: 6129–6133 (2008).
- Kagarise RE, *J Am Chem Soc* **77**:1377–1379 (1955).
- Baum J and Pines A, *J Am Chem Soc* **108**:7447–7454 (1986).
- Saalwächter K, *Prog Nucl Magn Reson Spectrosc* **51**:1–35 (2007).
- Lange F, Schwenke K, Kurakazu M, Akagi Y, Chung U, Lang M et al., *Macromolecules* **44**:9666–9674 (2011).
- Golitsyn Y, Pulst M, Samiullah MH, Busse K, Kressler J and Reichert D, *Polymer* **165**:72–82 (2019).
- Saalwächter K, *J Am Chem Soc* **125**:14684–14685 (2003).
- Saalwächter K, Multiple-quantum NMR studies of anisotropic polymer chain dynamics, in *Modern Magnetic Resonance*, ed. by Webb GA. Springer, Cham, pp. 1–28 (2017).
- Samiullah MH, Reichert D, Zinkevich T and Kressler J, *Macromolecules* **46**:6922–6930 (2013).
- Jiang A, Hussain H and Kressler J, *Macromol Mater Eng* **300**:181–190 (2015).
- Hu Y, Liu Y, Qi X, Liu P, Fan Z and Li S, *Polym Int* **61**:74–81 (2012).
- Lehner E, Gündel D, Liebau A, Plontke S and Mäder K, *Int J Pharm X* **1**: 100015 (2019).